

Crosslinked Coating Improves the Signal-to-Noise Ratio of Iron Oxide Nanoparticles in Magnetic Particle Imaging (MPI)

Sonja Horvat,^[a] Patrick Vogel,^[b] Thomas Kampf,^[b, c] Andreas Brandl,^[d] Aws Alshamsan,^[e, f] Hisham A. Alhadlaq,^[e, g] Maqsood Ahamed,^[e] Krystyna Albrecht,^[a] Volker C. Behr,^[b] Andreas Beilhack,^[d] and Jürgen Groll*^[a]

Abstract: Magnetic particle imaging is an emerging tomographic method used for evaluation of the spatial distribution of iron-oxide nanoparticles. In this work, the effect of the polymer coating on the response of particles was studied. Particles with covalently crosslinked coating showed improved signal and image resolution.

Magnetic particle imaging (MPI) is a novel tomographic method used for determination of the spatial distribution of superparamagnetic iron oxides (SPIOs). It is shown that MPI is capable of making high-resolution images of distribution of SPIOs

accumulated in lungs, blood vessels and cancer tissues, and recently it has been even used to image brain on a human scale with high precision and sensitivity.^[1]

MPI is based on the non-linear response of SPIOs magnetization to time-varying magnetic fields and provides direct access to information about the local concentration of SPIOs, which is not possible by magnetic resonance imaging (MRI). For imaging, a strong gradient in the form of a field-free point (FFP) or field-free line (FFL) is rapidly moved through the field of view (FOV) collecting successively MPI signal from SPIOs utilizing the fact that only in the vicinity of FFP or FFL MPI signal is generated. Traveling wave MPI used in this study provides a FOV enabling scanning probes with the size of small rodents with high temporal and spatial resolutions and high sensitivities.^[2,3]

Besides hardware design, the spatial resolution in MPI depends strongly on the SPIOs.^[3,4] To evaluate the suitability of nanoparticle system for imaging, magnetic particle spectroscopy (MPS) is usually employed. In comparison to MPI, MPS gives more specific information about the particle system, because of the absence of a gradient required for spatial encoding.^[5] Larger crystallites have larger magnetic moments resulting in a steeper magnetization curve, which led to a spectrum of higher harmonics with higher amplitudes.^[6]

Besides optimization of the core size for imaging, SPIOs require a coating to ensure stability and biocompatibility for pre-clinical and clinical applications,^[7] which might impact their physical properties and, therefore, image resolution. It has been shown that crosslinking of a coating to a hydrogel-like network significantly improved relaxivity of SPIOs in MRI,^[8] but the impact of the crosslinking of polymer coating of SPIOs in MPI has not been studied to our knowledge so far.

This study reports on the preparation of iron oxide nanoparticles as biocompatible tracers for MPI and evaluates the influence of particle coating, especially crosslinked versus non-crosslinked coatings, on signal intensity in MPS and image resolution in MPI.

Firstly, SPIOs with size of $18 \text{ nm} \pm 4 \text{ nm}$ were synthesized by thermal decomposition of an iron-oleate complex (SI, Figure S1–S2).^[9]

Subsequently, particles were coated by poloxamer Pluronic F127 (PF127) to render them water-dispersible (Figure 1). In addition, PF127 was modified with acrylate groups (PF127DA, Figure S3) to enable the conjugation of polymers containing thiol groups.

[a] S. Horvat, Dr. K. Albrecht, Prof. Dr. J. Groll
Department for Functional Materials in Medicine and Dentistry and
Bavarian Polymer Institute
University of Würzburg
Pleicherwall 2, 97070 Würzburg (Germany)
E-mail: juergen.groll@fmz.uni-wuerzburg.de

[b] Dr. P. Vogel, Dr. T. Kampf, Dr. V. C. Behr
Experimental Physics V
University of Würzburg
97074 Würzburg (Germany)

[c] Dr. T. Kampf
Institute of Diagnostic and Interventional Neuroradiology
University Hospital Würzburg
97080 Würzburg (Germany)

[d] Dr. A. Brandl, Prof. Dr. A. Beilhack
Department of Medicine II
Center for Experimental Molecular Medicine
Würzburg University Hospital
97080 Würzburg (Germany)

[e] Prof. Dr. A. Alshamsan, Dr. H. A. Alhadlaq, Prof. Dr. M. Ahamed
King Abdullah Institute for Nanotechnology
King Saud University
11451 Riyadh (Saudi Arabia)

[f] Prof. Dr. A. Alshamsan
Department of Pharmaceutics
College of Pharmacy
King Saud University
11451 Riyadh (Saudi Arabia)

[g] Dr. H. A. Alhadlaq
Department of Physics and Astronomy
College of Science
King Saud University
11451 Riyadh (Saudi Arabia)

Supporting information for this article is available on the WWW under
<https://doi.org/10.1002/cnma.202000009>

© 2020 The Authors. Published by Wiley-VCH Verlag GmbH & Co. KGaA.
This is an open access article under the terms of the Creative Commons
Attribution Non-Commercial NoDerivs License, which permits use and dis-
tribution in any medium, provided the original work is properly cited, the use
is non-commercial and no modifications or adaptations are made.

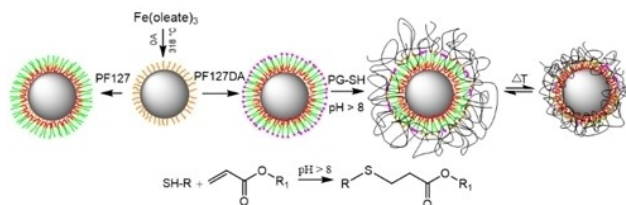


Figure 1. Schematic diagram of preparation of thermo-responsive SPIOs.

After phase transfer using PF127DA, conjugation of biocompatible thiol functionalized poly(glycidol)s (PG-SH) to the PF127DA coating on the SPIO surface was achieved by thiol-acrylate Michael addition,^[10,11] and coating identity was evaluated by Fourier transform infrared spectroscopy (Figure S4).

The hydrodynamic diameter determined by dynamic light scattering (DLS) was around 180 nm at 25 °C, suggesting aggregation.^[11] However, higher diameters of SPIOs coated with PF127 than expected were reported previously.^[12] Furthermore, the flat arrangement of particles in STEM images (Figure 2) indicated that capillary forces during drying lead to apparent aggregation, but that those were not permanent in the solution. Therefore, we assumed that if aggregation in solution occurred, it was rather transient than permanent.

Particles showed thermo-responsive behavior, which was monitored by DLS. PF127DAPG SPIOs incubated from 4 °C to 41 °C decreased almost by two-fold and this change became most evident between 4 °C and 25 °C. On the other hand, shrinkage of SPIO coated only with PF127 was much lower in

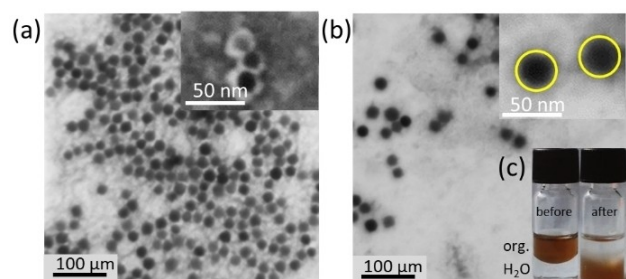


Figure 2. STEM analysis of (a) PF127 and (b) PF127DAPG SPIOs. (c) After phase transfer particles are completely dispersible in water.

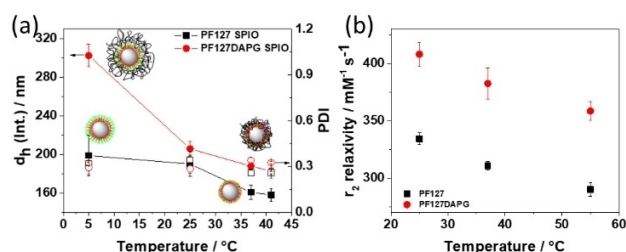


Figure 3. Swelling behaviour of (a) copolymer coated SPIOs. Full and empty symbols stand for dh and polydispersity (PDI), respectively. (b) Influence of temperature on the relaxivity r2 of particles measured at 7 T.

the same temperature range (Figure 3a). As a control, PF127DA coated SPIOs were also analyzed. The swelling of these nanoparticles resembled the swelling behavior of PF127 SPIOs (Figure S5). Similar behavior was observed of unloaded nanogels (hydrogel nanoparticles) and micelles composed only of the respective polymers (SI, Figure S5).

A change of swelling ratio for micellar structures of PF127 crosslinked with polymers such as heparin or polyethyleneimine was observed before.^[13] The higher thermo-responsiveness was explained by the hydrophobicity changes in the micellar structures and by electrostatic interactions between polymers. Reportedly, NP size changed up to 200 times in micellar constructs by varying temperatures from 4 – 37 °C when polymers were used that contained both hydrophobic and hydrophilic regions.^[13] As it is known that thiol modification renders PGs more amphiphilic,^[14] aside from a better swelling through the hydrophilic PG, the amphiphilicity might in a similar manner imply that the PF127DAPG coating could also exhibit sufficient hydrophobic interactions for a pronounced de-swelling above the lower critical solution temperature.

MRI was firstly employed to evaluate magnetic properties of particles. The transverse relaxivity r2, as the ability of a contrast agent to alter T2, was determined at different temperatures (Figure 3, Table S1). The transverse relaxivity r2 at 7 T of both types of SPIOs was significantly higher (330 mM⁻¹ s⁻¹ and 410 mM⁻¹ s⁻¹ for PF127 and PF127DAPG SPIOs, respectively, measured at 25 °C) than relaxivity of commercially available products such as Ferumoxitol (Feraheme, 68 mM⁻¹ s⁻¹, 7 T).^[15] The higher transverse relaxivity of our samples could be attributed to possible transient aggregation of particles in solution^[16] as well as to the larger core size of the nanocrystals in comparison to ultra-small particles in commercial products. Apart from the core size, the coating could have a great impact on the relaxivity of SPIOs. Coating permeability and thickness influence water diffusion to the SPIO surface and therefore particle MRI performance.^[17] As PF127 SPIOs coating was comprised of poloxamer assemblies with the OA due to hydrophobic-hydrophobic interactions, while PF127DAPG layer on SPIOs was based on the crosslinked polymeric network, it probable that a hydrogel-like crosslinked polymeric network around SPIOs was more water permeable than the layer of PF127.^[8,18] Further, elevated temperatures decreased the relaxivity of both samples, and this change was greater for the PGPF127DAPG SPIOs. At higher temperatures, polymers collapsed and were closer to the particle surface. In the case of the PF127DAPG SPIOs, this contraction led to higher polymeric network density as compared to the PF127 SPIOs due to the presence of both PG and PF127. This suggested that with increased temperature, reduction of diffusive accessibility of water led to the decrease of relaxivity.^[19]

Suitability of nanoparticles for MPI was analyzed firstly by MPS (Figure 4a–c). The decay of spectra of higher harmonics decreased with rising temperatures (Figure 4a,b), which might be attributed to the temperature-dependent change in viscosity of surrounding media.^[20] However, decays of spectra of higher harmonics of PF127DAPG and PF127 SPIOs markedly differed

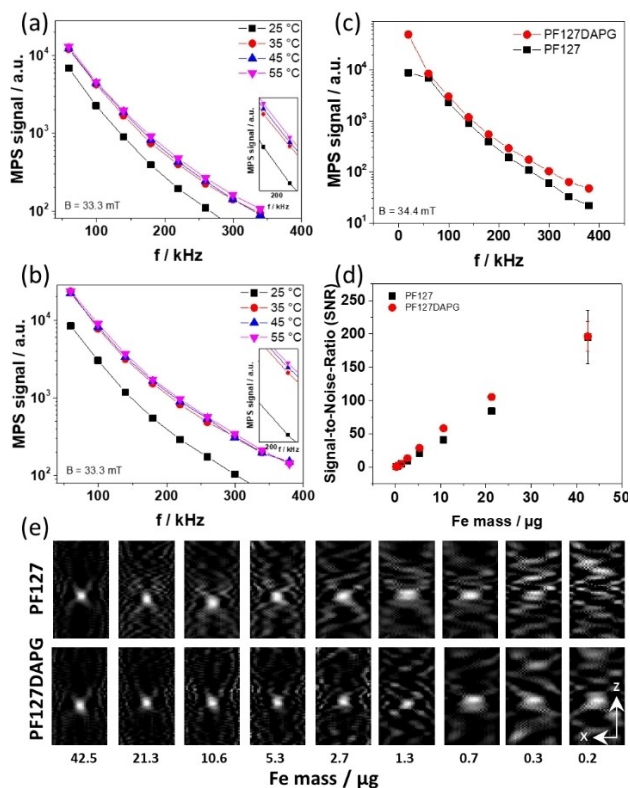


Figure 4. (a) Influence of temperature on MPS performance of PF127 and (b) PF127DAPG SPIOs. (c) Higher response of PF127DAPG SPIOs in MPS measured at 25 °C and (d) improved signal-to-noise ratio in MPI. (e) MPI images of PF127 and PF127DAPG SPIOs.

for PF127DAPG SPIOs (Figure 4c) which performed better, although both systems contained the same magnetic cores.

Similarly, PF127DAPG SPIOs displayed a superior signal-to-noise (SNR) ratio in comparison to PF127 (Figure 4d), when the same amount of SPIOs was used. Consequently, images with higher SNR resulting in a higher spatial resolution were obtained for PF127DAPG SPIOs in MPI (Figure 4e), where 5.3 μg of iron amount in PF127 SPIOs gave the same resolution as 1.3 μg of iron in PF127DAPG SPIOs. This outcome could be attributed to the differences in the coating between two types of particles. Usually, the optimization of tracers for MPIs is based on the optimization of the core size, whereas coating is considered important only for the *in-vivo* studies.^[21] Our study, however, implicates that particle coating might have an essential influence on the MPI performance and should not be neglected during the optimization of the tracers.

Finally, crosslinking of coating did not only improve r_2 in MRI, the signal in MPS and resolution in MPI but also cytocompatibility (Figure 5). Coating of SPIOs by PF127 showed cytotoxicity probably due to its high amphiphilic nature, which can lead to the solubilization of the lipids from the cell membrane.^[22] The presence of the biocompatible PG on the surface of SPIOs prevented PF127 dissociation and lowered the cytotoxicity of particles. PF127DAPG SPIOs did not induce any toxicity on healthy human fibroblasts and malignant plasma cells (Figure 5). These results, therefore, suggest that

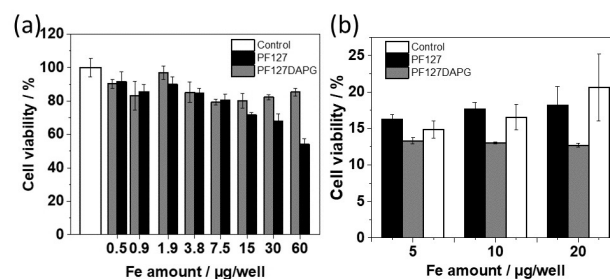


Figure 5. Cell toxicity studies of PF127 and PF127DAPG SPIOs on (a) healthy fibroblasts and (b) malignant plasma cells.

PF127DAPG SPIOs have high potential to be used in diagnostics.

In summary, this study demonstrates that crosslinking of the polymeric coating improved SPIO performance in MPI, MPS and MRI and highlights the importance of SPIOs coating for their application in imaging. Our study shows that the type of coating besides the iron oxide core size should not be neglected in the optimization of the SPIOs. Lastly, as crosslinking of the polymeric network on the surface of SPIOs with biocompatible PGs did not result in cytotoxicity, these tracers hold great promise for the application in diagnostics.

Author Contributions

S.H. designed and performed nanoparticle preparation, coating and characterization, analyzed the data and wrote the paper. K.A and J.G. conceived the experimental design, supported data analysis and writing of the paper. P.V., T.K, V.C.B. designed, performed and analyzed the MRI, MPS and MPI measurements. A.Br. and A.Be. conceived the biological experiments, analyzed the data and supported the writing. A.A., H.A.A., M.A. contributed with expertise on SPION synthesis and characterization and experimental design.

Acknowledgements

This project was supported by NanoCancer, a joined research program of King Saud University, Riyadh and the University of Würzburg, Germany.

Conflict of Interest

The authors declare no conflict of interest.

Keywords: crosslinked coating · imaging agents · magnetic properties · MPI · MPS

- [1] M. Graeser, F. Thieben, P. Szwargulski, F. Werner, N. Gdaniec, M. Boberg, F. Griese, M. Möddel, P. Ludewig, D. van de Ven, O. M. Weber, O. Woywode, B. Gleich, T. Knopp, *Nat. Commun.* **2019**, *10*, 1936.
- [2] a) P. Vogel, M. A. Rückert, P. Klauer, W. H. Kullmann, P. M. Jakob, V. C. Behr, *IEEE Transactions on Medical Imaging* **2014**, *33*, 400–407; b) P. Vogel, M. A. Rückert, S. J. Kemp, A. P. Khandhar, R. M. Ferguson, S. Herz, A. Vilter, P. Klauer, T. A. Bley, K. M. Krishnan, V. C. Behr, *IEEE Trans. Magn.* **2019**, 1–7.
- [3] a) P. Vogel, S. Lother, M. A. Rückert, W. H. Kullmann, P. M. Jakob, F. Fidler, V. C. Behr, *IEEE Transactions on Medical Imaging* **2014**, *33*, 1954–1959; b) P. Vogel, M. A. Rückert, P. Klauer, W. H. Kullmann, P. M. Jakob, V. C. Behr, *Phys. Med. Biol.* **2016**, *61*, 6620.
- [4] a) B. Gleich, J. Weizenecker, *Nature* **2005**, *435*, 1214; b) T. Knopp, N. Gdaniec, M. Möddel, *Phys. Med. Biol.* **2017**, *62*, R124–R178; c) D. Bobo, K. J. Robinson, J. Islam, K. J. Thurecht, S. R. Corrie, *Pharm. Res.* **2016**, *33*, 2373–2387.
- [5] a) K. Wu, D. Su, R. Saha, D. Wong, J.-P. Wang, *J. Phys. D* **2019**, *52*, 173001; b) S. Biederer, T. Knopp, T. F. Sattel, K. Lüdtke-Buzug, B. Gleich, J. Weizenecker, J. Borgert, T. M. Buzug, *J. Phys. D* **2009**, *42*, 205007.
- [6] a) N. Löwa, P. Knappe, F. Wiekhorst, D. Eberbeck, A. F. Thünemann, L. Trahms, *J. Magn. Magn. Mater.* **2015**, *380*, 266–270; b) L. W. E. Starmans, D. Burdinski, N. P. M. Haex, R. P. M. Moonen, G. J. Strijkers, K. Nicolay, H. Grull, *PLoS One* **2013**, *8*, e57335–e57335.
- [7] a) X. Li, J. Wei, K. E. Aifantis, Y. Fan, Q. Feng, F.-Z. Cui, F. Watari, *J. Biomed. Mater. Res. Part A* **2016**, *104*, 1285–1296; b) R. Hufschmid, H. Arami, R. M. Ferguson, M. Gonzales, E. Teeman, L. N. Brush, N. D. Browning, K. M. Krishnan, *Nanoscale* **2015**, *7*, 11142–11154.
- [8] C. Paquet, H. W. de Haan, D. M. Leek, H.-Y. Lin, B. Xiang, G. Tian, A. Kell, B. Simard, *ACS Nano* **2011**, *5*, 3104–3112.
- [9] J. Park, K. An, Y. Hwang, J.-G. Park, H.-J. Noh, J.-Y. Kim, J.-H. Park, N.-M. Hwang, T. Hyeon, *Nat. Mater.* **2004**, *3*, 891.
- [10] a) W. Zhu, B. Wang, Y. Zhang, J. Ding, *Eur. Polym. J.* **2005**, *41*, 2161–2170; b) A. V. Bordini, M. V. Lombardo, A. Wolosiuk, *RSC Adv.* **2016**, *6*, 77410–77426.
- [11] M. Theerasilp, W. Sungkarat, N. Nasongkla, *Bull. Mater. Sci.* **2018**, *41*, 42.
- [12] a) M. Gonzales, K. M. Krishnan, *J. Magn. Magn. Mater.* **2007**, *311*, 59–62; b) T. K. Jain, S. P. Foy, B. Erokwu, S. Dimitrijevic, C. A. Flask, V. Labhassetwar, *Biomaterials* **2009**, *30*, 6748–6756.
- [13] a) W. G. Zhang, K. Wu, L. Bahadur, R. K. C. Moss, M. A. Wang, Q. Lu, X. He, *ASC Nano* **2010**, *4*, 6757–6759; b) K. H. Bae, Y. Lee, T. G. Park, *Biomacromolecules* **2007**, *8*, 650–656; c) S. H. Choi, S. H. Lee, T. G. Park, *Biomacromolecules* **2006**, *7*, 1864–1870.
- [14] I. Zilkowski, I. Theodorou, K. Albrecht, F. Ducongé, J. Groll, *Chem. Commun.* **2018**, *54*, 11777–11780.
- [15] H. Wei, O. T. Bruns, M. G. Kaul, E. C. Hansen, M. Barch, A. Wiśniowska, O. Chen, Y. Chen, N. Li, S. Okada, J. M. Cordero, M. Heine, C. T. Farrar, D. M. Montana, G. Adam, H. Ittrich, A. Jasanoff, P. Nielsen, M. G. Bawendi, *Proc. Natl. Acad. Sci. USA* **2017**, 201620145.
- [16] L. Li, W. Jiang, K. Luo, H. Song, F. Lan, Y. Wu, Z. Gu, *Theranostics* **2013**, *3*, 595–615.
- [17] a) S. Tong, S. Hou, Z. Zheng, J. Zhou, G. Bao, *Nano Lett.* **2010**, *10*, 4607–4613; b) L. E. W. LaConte, N. Nitin, O. Zurkiya, D. Caruntu, C. J. O'Connor, X. Hu, G. Bao, *J. Magn. Reson. Imaging* **2007**, *26*, 1634–1641; c) J. C. Park, G. T. Lee, H.-K. Kim, B. Sung, Y. Lee, M. Kim, Y. Chang, J. H. Seo, *ACS Appl. Mater. Interfaces* **2018**, *10*, 25080–25089.
- [18] Y. Lin, S. Wang, Y. Zhang, J. Gao, L. Hong, X. Wang, W. Wu, X. Jiang, *J. Mater. Chem. B* **2015**, *3*, 5702–5710.
- [19] N. Izza Taib, V. Agarwal, N. M. Smith, R. C. Woodward, T. G. St Pierre, K. S. Iyer, *Mater. Chem. Front.* **2017**, *1*, 2335–2340.
- [20] S. Draack, T. Viereck, C. Kuhlmann, M. Schilling, F. Ludwig, *International Journal on Magnetic Particle Imaging* **2017**, *3*.
- [21] Y. Du, P. T. Lai, C. H. Leung, P. W. T. Pong, *Int. J. Mol. Sci.* **2013**, *14*, 18682–18710.
- [22] M. Gonzales, L. M. Mitsumori, J. V. Kushleika, M. E. Rosenfeld, K. M. Krishnan, *Contrast Media Mol. Imaging* **2010**, *5*, 286–293.

Manuscript received: January 2, 2020
 Revised manuscript received: February 14, 2020
 Accepted manuscript online: February 22, 2020
 Version of record online: April 1, 2020